Femtosecond Laser-Inscribed Non-Volatile Integrated Optical Switch in Fused Silica Based on Microfluidics-Controlled Total Internal Reflection

Ana Radosavljević ⓘ, Andres Desmet ⓘ, Jeroen Missinne ⓘ, Kumar Saurav, Vivek Panapakkam, Salvatore Tuccio, Cristina Lerma Arce, Jan Watté, Dries Van Thourhout ⓘ, and Geert Van Steenberge ⓘ

Abstract—We demonstrate a non-volatile optical power switch, fabricated by femtosecond laser inscription in a fused silica substrate, with switching operation based on microfluidics-controlled total internal reflection. The switch consists of crossed waveguides and a rectangular, high aspect ratio microfluidic channel, located at the waveguide crossing. The switching between total internal reflection and transmission at the channel wall is determined by the refractive index of the medium inside the channel. Femtosecond laser inscription allows for co-integration of low-loss optical waveguides and channels with smooth sidewalls and thus the fabrication of low insertion loss switches that are broadband and show low polarization dependent losses. The measured total internal reflection loss of the fabricated switch is about 1.5 dB at the wavelength 1550 nm. The loss due to transmission through the channel filled with refractive index matching liquid is about 0.5 dB. Detailed finite difference time domain and beam propagation method simulations of the switch's performance indicate that the losses can be further reduced by optimizing its geometry, together with further adjusting the inscription parameters.

Index Terms—Femtosecond laser inscription, fused silica, microfluidics, non-volatile integrated optical switch, single mode waveguides, total internal reflection.

Ana Radosavljević is with the Photonics Research Group, Department of Information Technology (INTEC), Centre for Microsystems Technology, the Department of Electronics and Information Systems (ELIS), Ghent University–IMEC, 9052 Gent, Belgium (e-mail: ana.radosavljevic@ugent.be).

Andres Desmet, Jeroen Missinne, and Geert Van Steenberge are with the Centre for Microsystems Technology, Department of Electronics and Information Systems (ELIS), Ghent University–IMEC, 9052 Gent, Belgium (e-mail: andres.desmet@ugent.be; Jeroen.Missinne@ugent.be; Geert.VanSteenberge@ugent.be).

Dries Van Thourhout is with the Photonics Research Group, Department of Information Technology (INTEC), Ghent University–IMEC, 9052 Gent, Belgium (e-mail: Dries.VanThourhout@ugent.be).

Kumar Saurav, Vivek Panapakkam, Salvatore Tuccio, Cristina Lerma Arce, and Jan Watté are with CommScope, 3010 Kessel-Lo, Belgium (e-mail: Saurav.Kumar@commscope.com; Vivek.Panapakkam@commscope.com; salvatore.tuccio@commscope.com; cristina.lermaarce@commscope.com; jan.watte@commscope.com).

I. INTRODUCTION

THE spreading of fiber-to-the-home (FTTH) technology, driven by the increasing amount of internet traffic over the past decade, requires the development of optical power switches (OPSs) for efficient optical network management. For instance, broadband OPSs are needed both in high- and low-port-count switch matrices for the management of fiber network infrastructure in access networks.

A lot of effort has been invested in developing integrated optical switches since they can be combined with other optical functions on a chip [1]. Integrated switches have been proposed in several different material platforms, using mechanisms such as the electro-optic and thermo-optic effect to induce small changes in refractive index or using thermal deformation to induce displacement of waveguides [2]–[4]. All proposed switches require a continuous power during operation which leads to increased energy consumption and network management costs.

Recently, microfluidic silicon photonic integrated OPSs have been proposed as a new class of non-volatile, easily (remotely) reconfigurable switches that could increase the flexibility of a network and help reduce the maintenance costs [5]–[8]. As the switching state is controlled by microfluidics, the OPS needs to be powered only when it needs to be reconfigured. Compared to existing switch concepts, these devices offer very low static power consumption, broadband operation, no moving mechanical parts and high reliability.

In this work, we demonstrate a microfluidic controlled non-volatile OPS in a low refractive index (RI) contrast waveguide platform in fused silica based on femtosecond laser inscription (FLI) [9]–[11]. Exposing fused silica to tightly focused femtosecond laser pulses results in a permanent local modification of the optical and chemical properties of the glass in the focal volume of the laser beam. More specifically, the modified regions in the glass have an increased RI and can be selectively removed using wet chemical etching. The modification is induced by nonlinear multiphoton absorption processes [10], [11]. The increased RI allows for femtosecond laser direct writing (FLDW) of waveguides in fused silica. These waveguides can have low and nearly polarization independent propagation losses and mode field diameters (MFDs) comparable to single mode fibers (SMFs) at telecom wavelengths [10], [11], which makes them suitable for low insertion loss photonic integrated
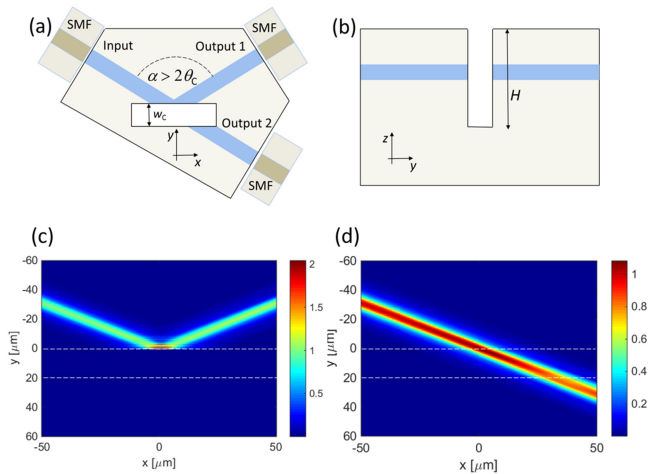
Fig. 1. (a) Scheme of the switch with edge coupled single mode fibers–top view, (b) cross-section of the switch, Normalized electric field amplitude in (c) TIR state and (d) transmission state obtained with BPM simulations for the angle between waveguides $\alpha = 116°$ and the channel width 20 μm. White dashed lines in (c) and (d) mark the positions of the channel walls.

circuits with easier packaging and without the need for polarization diverse design, as opposed to silicon photonic integrated circuits [12].

Fused silica is one of the few materials for which it has been demonstrated that direct exposure to femtosecond laser pulses leads to a locally increased wet chemical etching rate [9]. Translating the sample through the focus of a femtosecond laser beam can be used to directly define surface reaching or buried 3D microfluidic channels with arbitrary shapes which are formed by subsequent selective wet chemical etching of the exposed volumes in aqueous solutions of potassium hydroxide (KOH) or hydrofluoric acid (HF).

The compatibility of FLDW and femtosecond laser induced chemical etching (FLICE) technologies allows for simultaneous inscription of photonic circuits, as well as microfluidic and fiber alignment structures, integrated on a single substrate with sub-micron alignment precision [9]. Since FLI does not require any mask or post-development steps, it is a suitable technique for rapid prototyping of photonic and microfluidic devices (reduced operational expenditure). Moreover, fused silica is a very attractive material platform for integrated photonics and microfluidics since it is optically transparent at visible and telecom wavelengths, stable in time, chemically inert, nonporous, hydrophilic and it has a low temperature expansion coefficient [9].

The switching operation of the femtosecond laser inscribed non-volatile OPS in fused silica demonstrated in this work is based on microfluidics-controlled total internal reflection (TIR). The switch consists of crossed single mode waveguides and a microfluidic channel at the waveguide crossing (Fig. 1(a)) inscribed in the same laser exposure step. The switching between total reflection and transmission at the channel wall is determined by the refractive index of the medium inside the channel. After the laser inscription, the channel is formed by subsequent etching in KOH, which is more selective towards the irradiated channel's volume than HF [13], thus allowing for fabrication of channels

with a better controlled width and vertical walls necessary for good angular alignment between the waveguides and the TIR mirror. To avoid etching the waveguides, sufficient unexposed space is left between the channel and the waveguides. Compared to the fabrication of TIR switches in silica planar lightwave circuits, which consists of several steps including conventional lithographic processes [14]–[16], FLI allows for faster and more robust fabrication. Filling and removing the liquid from the channel can be done by electrowetting on dielectric (EWOD) [5], using bubble actuation [14]–[16] to push the liquid out of the channel, or using a micropump.

The paper is organized as follows: in Section II the initial design considerations for the OPS are given, while in Section III the influence of possible sources of loss on the optical performance of the switch is evaluated and the design parameters are adjusted to counteract some of the possible losses. In Section IV, the fabrication of the switches is described in detail, followed by characterization and measurements results in Section V. The paper is concluded in Section VI.

II. WORKING PRINCIPLE AND INITIAL DESIGN REQUIREMENTS

The structure and working principle of the microfluidics controlled digital optical power switch in fused silica are illustrated in Fig. 1. The light is transmitted through the surface reaching channel if the channel is filled with a liquid with RI matched to the RI of the waveguides. Switching the light to the crossing waveguide is realized by TIR at the channel wall when the liquid is removed from the channel.

In order to capture the reflected light at the channel wall in the crossing waveguide, the input and crossing waveguide should form an angle $\alpha > 2\theta_C$, where θ_C is a critical angle for TIR at the waveguide/air interface. The extracted peak refractive index (RI) change induced by the femtosecond laser pulses in this work is $\Delta n \sim 5 \times 10^3$, as will be shown later in Section IV. This is within the range of typically reported values of the order $10^4 - 10^3$ [10], [11], [16]. Since Δn is low, the effective index of the mode can be approximated with the index of unmodified fused silica $n_s = 1.444$ at the wavelength $\lambda = 1550$ nm for the initial estimation of the critical angle for TIR:

$$\theta_C = \arcsin\left(\frac{1}{n_S}\right) = 43.83°. \tag{1}$$

This condition is valid for an infinite plane wave incident under a single angle at the fused silica/air interface. Since the light in the single mode waveguides propagates as a mode with a finite width and an approximately Gaussian field distribution, the waveguide mode is incident at the interface under a range of angles defined by the numerical aperture of the waveguides. In order to minimize the losses in the TIR state of the switch, this should be taken into account and the waveguide should be placed under an angle for which the TIR condition is satisfied for the entire range of incident angles. We use 3D finite-difference time-domain (FDTD Lumerical) simulations, assuming TE light polarization, to determine the minimal angle between the waveguides necessary for efficient total internal reflection, in the case of $\Delta n = 5 \times 10^3$. FDTD is a numerical method which
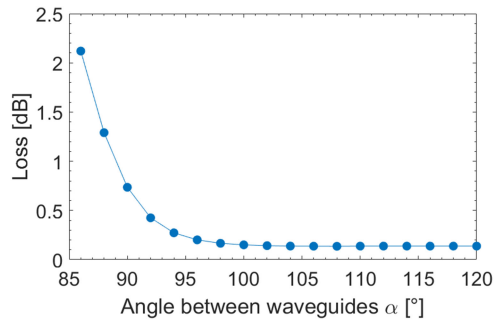
Fig. 2.   Simulated loss in the reflection state of the switch (air in the channel) as a function of the angle between crossed waveguides.
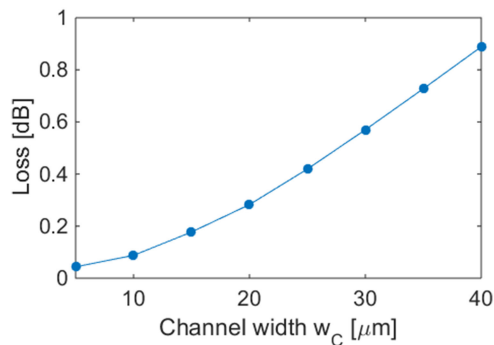

Fig. 3.   Simulated loss in the transmission state of the switch (index matched liquid in the channel) as a function of the channel width. The angle between the crossed waveguides is fixed to $\alpha = 116°$.

directly solves the time-dependent Maxwell's equations without approximations and can be used to highly accurately model light propagation in the case of sharp light turning due to TIR. The waveguide dimensions are estimated to be 8 μm from the microscope images of fabricated waveguides. The sidewall of the channel in the simulations is aligned with the crossing point of the center of the input and first output (output 1) waveguide. The results in Fig. 2 show that a loss below 0.3 dB in the TIR state can be obtained when the angle between the waveguides is above $\alpha = 94°$. Efficient TIR is necessary for both low loss at output 1 and low crosstalk at output 2 (see Fig. 1(a)).

When the channel is filled with index matching liquid, the light propagates without confinement through it. Therefore, increasing the channel width leads to higher losses due to divergence of the light beam. Fig. 3. shows the losses for light transmission through the channel as a function of the channel width for a fixed angle $\alpha = 116°$ between the crossed waveguides. The minimal channel width considered in the simulations is 5 μm, which corresponds to minimal achievable channel width with the femtosecond laser inscription system used in our work, as will be shown in Section IV. The maximal channel width in the simulations is set to 40 μm which is below the Rayleigh range $z_R = 46.25$ μm of an approximately Gaussian waveguide mode with mode field diameter 11.5 μm. This MFD is measured for the waveguides fabricated in our work. A channel width below 20 μm results in a loss lower than 0.3 dB at output 2.

The transmission results in Fig. 3 are obtained with 3D finite-difference beam propagation method (BPM) implemented in software from Synopsys (RSoft BeamPROP). BPM is a widely used numerical method for fast simulations of light propagation based on solving the Helmholtz equation in the paraxial approximation, which makes it ideal for simulations of low RI contrast waveguides. However, its accuracy for off-axis light propagation decreases with increasing the angle under which the light propagates with respect to the axis. In the simulations of the TIR switch, the axis of propagation is set parallel to the channel's wall. Therefore, the light propagates closer to the axis when the angle α between crossed waveguides is increased. For large enough angle $\alpha > 115°$, the difference in results obtained by 3D BPM and 3D FDTD in this work is less than 2%. Therefore, the remainder of the simulation results in Sections II and III are obtained with BPM for large enough fixed angle $\alpha = 116°$ to benefit from the shorter computation time compared to FDTD. The choice of a large angle α for the TIR switch will be further elaborated in Section III.

The above numerical results demonstrate the feasibility of low loss light switching in the proposed femtosecond laser written TIR switch in fused silica. The switch can be fabricated with losses at output 1 (air in channel) and output 2 (RI matched liquid in channel) lower than 0.3 dB for a broad range of angles between crossed waveguides $\alpha > 94°$ and a channel width up to 20 μm, which is achievable using FLI. In the next section the influence of possible fabrication imperfections on the loss and the isolation of the TIR and transmission state of the switch will be discussed.

III. Numerical Analysis of the Optical Performance

There are several loss mechanisms associated with each state of this switch. For the TIR state, the optical loss can be caused by scattering due to surface roughness at the channel sidewall, the vertical channel sidewall angle, or angular or lateral misalignment between the channel and waveguide crossing. When the switch is in the transmission state, losses arise from the Fresnel reflections and refraction due to possible RI mismatch between the waveguides and the liquid in the channel, which can be in random directions due to the roughness of the channel walls, and from the divergence of the beam in the channel as explained above. In this section, the various optical loss contributions will be evaluated for an estimation of the switch performance at the wavelength of 1550 nm and structural parameters of the TIR switch will be chosen in order to maximally suppress some of these losses.

A. Angular Misalignment

Angular misalignment between the waveguides and the channel can induce significant losses in the TIR state of the switch, since the waveguides have low numerical aperture (NA). For the RI contrast $\Delta n = 5 \times 10^3$, the waveguides have NA ≈ 0.11 and acceptance angle 12.35°. Angular misalignment can occur in the xy plane, which is indicated with red dashed lines in Fig. 4(a) or in the yz plane due to non-vertical channel walls, which is schematically presented in Fig. 4(b).
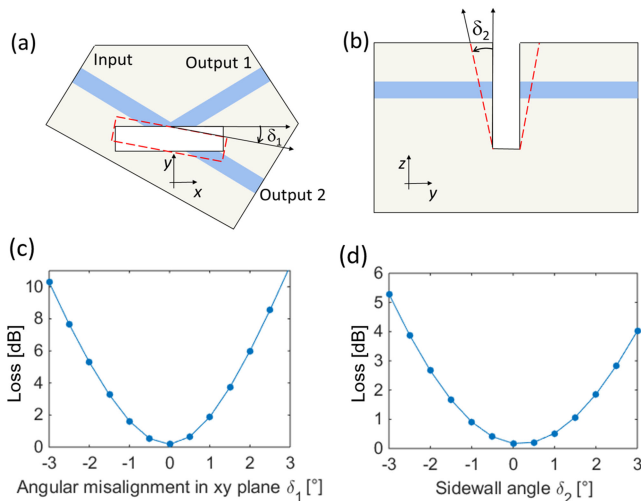
Fig. 4. Schematic representation of angular misalignment in (a) xy plane and (b) yz plane. Positive misalignments are indicated with arrows. Simulated losses at the output 1 due to angular misalignment in (c) xy plane and (d) yz plane. The angle between the crossed waveguides is fixed to $\alpha = 116°$.
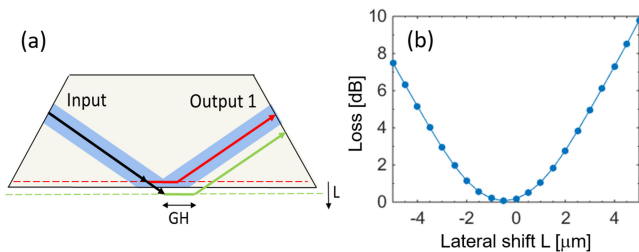

Fig. 5. (a) Schematic representation of light reflection due to lateral misalignment of the channel. GH stands for the Goos–Hänchen shift. Lateral shift of 0 μm corresponds to position of the channel sidewall exactly at the crossing point of the center of both waveguides. Arrow indicates positive lateral misalignment. (b) Simulated losses at the output 1 of the switch due to the lateral misalignment L. The angle between the waveguides is set to $\alpha = 116°$.

Fig. 4 shows the losses simulated with 3D BPM due to the misalignment in the *xy* plane (Fig. 4(c)) and due to the channel sidewall angle (Fig. 4(d)). Both a misalignment in the *xy* plane of more than $\pm1°$ or a sidewall angle of more than $\pm1.5°$ could lead to losses higher than 1 dB. Using FLI to write waveguides and define channel in the same laser exposure step and using subsequent KOH etching to form the channel can help keep the angular misalignments below $1°$ in both planes. More details will be given in the Section IV.

B. Lateral Misalignment

Lateral misalignment represents the misalignment between the channel wall and the waveguide crossing (illustrated with red and green dashed line in Fig. 5(a)). Shifting the channel wall about 0.5 μm towards the waveguide crossing results in maximized TIR efficiency since it compensates the Goos–Hänchen shift at the interface [18]. If the channel wall is shifted further towards the waveguides or away from the waveguide crossing, the position of output 1 is not aligned with the light reflected at the interface, as schematically presented in Fig. 5(a). This causes

increased loss at output 1 as shown in Fig. 5(b). A lateral shift of more than 2 μm towards the waveguide crossing or more than 1 μm away from the crossing results in losses above 1 dB.

C. Channel Sidewall Roughness

The etched surfaces of microfluidic structures fabricated by FLICE are typically not ideally smooth [19], [20]. Due to the surface roughness of the channel wall, the light beam is scattered when it is incident on the wall of the empty channel. This can lead to loss at output 1 in two ways. First, if the crossed waveguides are placed under an angle close to critical angle for TIR, light can be scattered under an angle for which the TIR condition is not valid anymore, resulting in loss at output 1 and possibly cross-talk at output 2 [21]. This can be partly prevented by placing the crossed waveguides under an angle sufficiently larger than the critical angle. Second, since the waveguides have a low RI contrast and a small acceptance angle, the power reflected to output 1 is very sensitive to the incident angle, as shown in Fig. 4. Hence scattering can cause excess loss compared to TIR at the perfectly smooth channel wall, since the incident angle is locally changed by the roughness. The roughness of the channel wall can be described by its root mean square (rms) deviation and the correlation length. In this work the rms of the roughness after FLICE is about 50 nm and the correlation length is about 2 μm as assessed from scanning electron microscope (SEM) images and measured with white light interferometry. The roughness described by these parameters could lead to a local random change of angle in the range of about $\pm$arctg (rms/correlation length) $\sim \pm1.4°$. Assuming that the waveguides are under a large enough angle α, the excess loss with respect to surface roughness is assumed to be of the order of 1 dB for output 1, based on the results for angular misalignment in Fig. 4.

Furthermore, the light scattered at the rough channel wall can be transmitted towards the output 2. Decreasing the channel width could increase the unwanted light coupling and crosstalk. Therefore, in attempt to minimize both insertion loss and cross-coupling for the experimental demonstration of the switch, the channel width is fixed to 20 μm.

D. Refractive Index Mismatch Between the Waveguides and the Liquid in the Channel

When the light is incident at the interface between two optically different and non-absorbing media, part of its power is reflected due to the Fresnel reflections and the rest is transmitted under an angle defined by Snell's law. Therefore, if the RI of the liquid which is used to transmit the light to output 2 is not matched to the RI of the waveguides, part of the light will be reflected and guided towards output 1, while the transmitted power will be refracted under an angle and thus not be perfectly aligned with the position of waveguide at output 2. This leads to losses at output 2 and crosstalk at output 1 (Fig. 6). In a femtosecond laser inscribed microfluidics switch, this RI mismatch can happen if the RI of the waveguide cannot be accurately extracted or if the temperature dependence of the RI of the liquid in the channel is significantly different from the temperature dependence of fused silica, which can lead to RI mismatch if the switch is used over
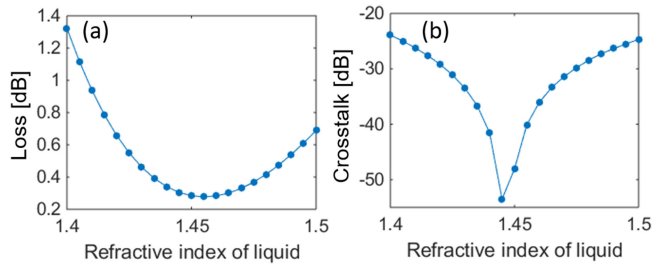
Fig. 6. Simulated losses at output 2 (a) and crosstalk at output 1 (b) as a function of refractive index of the liquid in the channel used for light transmission. The angle between the waveguides is fixed to $\alpha = 116°$ and the channel width is 20 μm.

TABLE I
DESIGN PARAMETERS FOR TIR SWITCH AT THE WAVELENGTH OF 1550 nm

Symbol	Quantity	Nominal value (Tolerance)
w_C	Channel width	20 μm (+0/-15 μm)
α	Angle between the waveguides	116° (+4/-10°)
L	Offset distance from the ideal lateral position	-0.5 μm (+1/-0.5 μm)
δ_2	Channel sidewall angle	0° (±0.5°)
δ_1	Horizontal angular mismatch (*xy* plane)	0° (< ±0.5°)
n	Refractive index of liquid used for transmission	1.449 (-1.5 %, +2.5 %)
H	Channel depth	>100 μm (+50/-20 μm)

broad temperature range. If the RI of the liquid is not matched to the waveguide, the position of the bar waveguide can be shifted to compensate for the refraction. However, as the RI mismatch increases, the isolation of output 1 decreases. Moreover, higher RI mismatch can lead to light scattering through the channel under a random range of angles when the channel wall is not ideally smooth and to higher loss at output 2.

E. Design Parameters for the Demonstration of the Switch

The TIR switch operation is very sensitive to several parameters as shown above. The nominal values of design parameters for the switch demonstration and their tolerances defined as deviations from nominal values that render losses up to 0.5 dB are listed in Table I. The minimal and maximal achievable height of the channel achievable with the FLI system used in our work will be discussed in Section IV.

IV. FEMTOSECOND LASER INSCRIPTION OF THE SWITCH

We use a commercial ytterbium-doped fiber laser (Satsuma, Amplitude Systèmes) to fabricate both microfluidic channels and single mode optical waveguides, integrated together on a single glass substrate. The lasing frequency is doubled from 1030 nm to 515 nm using a second harmonic generation (SHG) module to achieve more efficient laser processing of wide-bandgap fused silica by reducing the order of the multiphoton

TABLE II
LOSS CONTRIBUTIONS IN TIR SWITCH AT THE WAVELENGTH OF 1550 nm

Loss factor	Loss [dB]
Coupling loss between SMF-28 and waveguide with RI matched liquid	0.86
Total propagation loss in 1.7cm long waveguides	0.85
Reflection loss at the channel wall (air in channel)	1.5
Transmission loss through the channel filled with RI matched liquid	0.5

absorption [17]. Pulse width is <400 fs and the repetition rate is 500 kHz. The linearly polarized laser beam is focused onto a high purity 500 μm thick fused silica substrate from Siegert with a 0.6 NA aspheric lens (Newport 5722-A-H). The power of the femtosecond laser is controlled with an automated rotatable 1/2-wave plate and a linear polarizer. Average laser power ranging from 25 mW–350 mW are measured after focusing. The samples are placed on a computer-controlled motorized XY stage that is translated perpendicularly to the laser beam with a speed ranging from 0.01–10 mm/s.

In the following sub-sections, details of waveguide and channel fabrication as well as their co-integration for the fabrication of the optical switch will be described.

A. Fabrication of Microfluidic Channel

Using the described writing system in our work the cross-sectional dimensions of the single laser written track in the glass are of the order of a few μm, depending on the laser power and translation speed of the motorized stage. Since we want to fabricate 20 μm wide and >100 μm deep channel, we use a multi-scan technique to write a matrix of laser lines to expose the volume of the channel which is to be etched [19], [20]. The maximal depth of the channel is conditioned with the maximal focus depth in fused silica with acceptable spherical aberrations originating from the air/fused silica interface, which is about 140 μm for the inscription parameters used in this work. These aberrations can significantly disturb the intensity distribution in the laser focus spot and cause small variations in the channel width along the channel depth and thus the sidewall angle of the channel [22].

It has been suggested that the presence of internal stress surrounding the laser track lines is the main reason for the induced etching of the exposed glass [20]. The presence of adjacent multiple tracks can affect the etching process and the channel wall roughness after etching since the stress field and the material densification in the region of the previously written tracks can be perturbed by subsequently written tracks. Therefore, it is necessary to find the optimal separation of the tracks to ensure the complete etching of the channel and the lowest roughness of the channel wall.

We begin the optimization of the channel fabrication by writing a single column of laser lines stacked in height from bottom to the top in the 500 μm thick fused silica samples. Lines
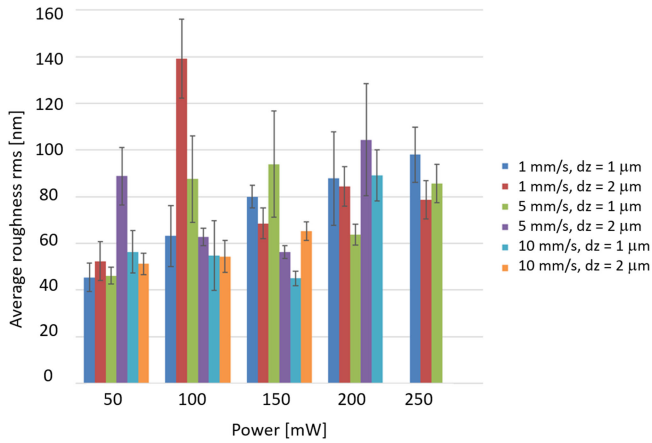
Fig. 7. Dependence of the wall average rms surface roughness after etching on the power of the femtosecond laser and the translation speed of the motorized stage. Average rms roughness is measured with white light interferometry.
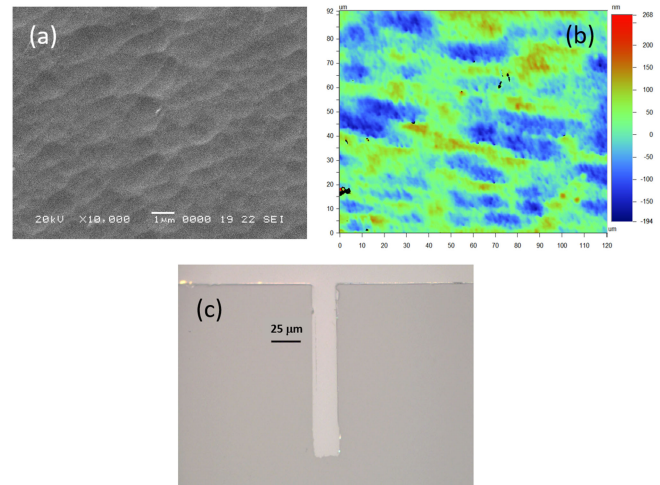

Fig. 8. (a) SEM image and (b) white light interferometry image of surface morphology after etching. (c) Cross-section of the channel showing vertical walls.

are written from bottom to top to avoid light scattering at already modified tracks. Different single line stacks are written with a vertical line separation of 1 μm and 2 μm, laser powers ranging from 25 mW to 250 mW and a stage translation speed from 1 mm/s to 10 mm/s. The femtosecond laser induced etch rate in fused silica is strongly dependent on the polarization of the writing beam. Thus, the laser lines are written perpendicularly to the laser polarization in order to benefit from the enhanced etching rate [19], [23]. Subsequently, the irradiated glass is etched in a 30% aqueous KOH solution [13]. The temperature of the KOH solution is kept at 85°C during the 4h long etching. We use magnetic stirring in order to keep the uniform temperature distribution in the solution. In this way channels with a minimal width of about 5 μm could be fabricated. Since etching of such narrow channels is not efficient when the irradiated volumes can only be etched from the top, we use mechanical dicing orthogonal to the laser tracks to expose the cross-sections and allow for etching from the sides as well. We would like to note that femtosecond laser could be used to make for e.g., access ports on the side of the narrow channels in the same exposure step instead of mechanical dicing to facilitate their etching [24], but this would significantly increase the laser exposure time. Therefore, for the purpose of this study we use mechanical dicing. After etching, the sidewall roughness is characterized using a white light based interferometry technique (Wyko) and the results are summarized in Fig. 7. The roughness is measured over areas of 100 μm $\times$ 100 μm. Power threshold for the etching is about 50 mW independent of the translation speed. Increasing the power further does not render significant changes in the average roughness but can lead to the emergence of micro-explosion sites, which can locally deteriorate the optical quality of the surface, similarly to findings in [19]. The lowest average rms roughness is just below 50 nm for the lowest translation speed of the motorized stage of 1 mm/s and the lowest laser power. We observed that the roughness rms increases above 100 nm for combined higher powers and the fastest translation speed 10 mm/s. However, this could not be measured accurately and is therefore not shown in Fig. 7.

Next, we use the parameters which give the lowest roughness, laser power of 50 mW and a 1 mm/s stage translation speed, for the multi-scan exposure of the channel. Similarly to vertical single line stacking, the horizontal layers were exposed from bottom to top in order to avoid scattering of the laser beam when passing through the already modified glass regions. It was found that track-to-track separations in horizontal and vertical direction $dy = dz = 2$ μm is sufficient to avoid deterioration of sidewall roughness after etching compared to vertically stacked single line laser tracks. A sidewall roughness with rms about 50 nm was measured after mechanically dicing through the channel to expose the walls (Fig. 8(b)). The roughness correlation length of ≈ 2 μm was estimated from a SEM image (Fig. 8(a)). Since the extent of the modified volume in glass after a single laser line exposure leads to a few μm width of the etched pattern, we found that 8 lines with a separation of 2 μm in the horizontal direction should be written to obtain about 20 μm wide channels for the chosen irradiation conditions. Therefore, the matrix of 8 $\times$ 70 laser tracks was written in order to fabricate a channel with the cross-sectional dimensions 20 μm $\times$ 140 μm.

The cross-section of the channel is exposed after dicing the sample perpendicularly to the channel. The shape of the cross-section was examined after it was polished to a high optical quality. The polishing was done after encapsulating the sample in an epoxy polymer which provides mechanical stability and prevents breaking off the channel edges during polishing. The sidewall angle of fabricated channel after etching in KOH is less than 1° as obtained from the microscope images (Nikon Eclipse) of the cross-section of the channel (Fig. 8(c)).

B. Waveguide Fabrication and Characterization

Detailed optimization of the waveguide inscription has been performed before fabrication of the switch. FLI parameters such as laser pulse energy and translation speed of the motorized stage have been varied in order to find the processing window for single mode optical waveguides with optimal characteristics

at telecom wavelengths: low propagation loss and mode profiles similar to the mode profile of single mode fibers to ensure low coupling losses. Since the waveguides have to be >40 μm below the surface of the fused silica substrate to achieve high enough RI difference for a MFD matched to SMF [25], [26], we write the waveguides 50 μm below the substrate surface.

The waveguide mode profiles are recorded by imaging the near field at the end-facet using an infrared camera (Xenics Xeva) coupled to a 100X infinity corrected objective (Nikon) after launching the light from a fiber coupled laser diode operating at 1550 nm (QPhotonics) to the waveguides through a single mode fiber (SMF-28). The mode field intensity profiles of the single mode fiber at 1550 nm is recorded as well using the same setup for calibration and comparison with the waveguide modes. We calculate the mode field diameters from the recorded mode intensity distributions using the $1/e^2$ method.

Propagation losses of the waveguides are obtained from the slopes of optical frequency domain reflectometry (OFDR) measurements of the waveguides. OFDR measurements are performed by launching light into the waveguides using the single mode fiber connected to a tunable laser source incorporated in the commercial OFDR device LUNA OVA 5000 [27] and using the provided software. We fabricate 10 cm long waveguides for the OFDR measurements and apply the RI matching liquid (RI = 1.46 at 589.3 nm (D line) from Cargille, series A) between input fiber and waveguide sample in order to minimize the reflections at the input [28]. The coupling losses are subsequently obtained by subtracting the propagation loss contribution from the total insertion loss of the waveguides. The optical power transmitted through the waveguides is measured after in-coupling light from a laser light source at the wavelength of 1550 nm (QPhotonics) and out-coupling it to an optical power meter (Newport 1930-C) through edge coupled single mode optical fibers at 1550 nm (SMF-28 from Corning). The total insertion loss of the waveguides is extracted from these power transmission measurements and a reference fiber–to–fiber transmission measurement. The RI matching liquid is applied between fibers for the reference transmission measurement and between fibers and waveguides for transmission measurements.

The orientation of the femtosecond laser polarization with respect to the writing direction of the waveguides affects the properties of the waveguides [29]. Therefore, the waveguides are written in parallel and perpendicular to the polarization of the femtosecond laser using the same writing parameters to compare the waveguide properties. The lowest loss single mode waveguides for both waveguide writing orientations with respect to the linear laser polarization are obtained for a writing speed 0.5 mm/s. The results in Fig. 9(a) show that the propagation losses are slightly lower when waveguides are inscribed in parallel to the laser polarization, as demonstrated in [29]. A propagation loss below 1 dB/cm can be obtained for a broad range of femtosecond laser power for both waveguide writing orientations. Decreasing the inscription laser power renders lower waveguide propagation loss but larger mode field diameter of the waveguide modes (Fig. 9(b)). We use a laser power of 155 mW for the inscription of the waveguides since it provides the lowest propagation loss for waveguide mode field diameter
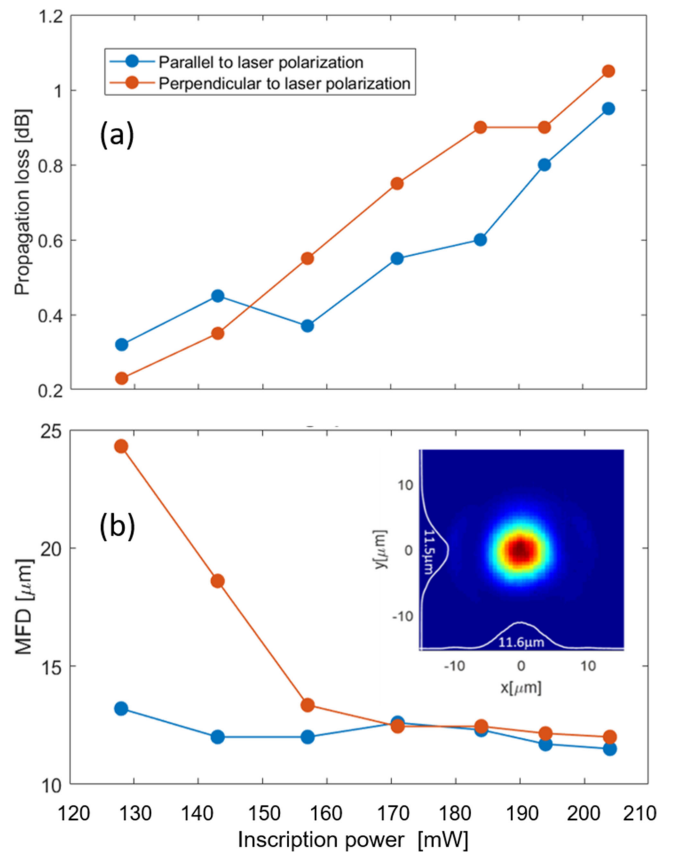

Fig. 9. Characteristics of waveguides written with speed 0.5 mm/s in parallel and perpendicularly to femtosecond laser polarization: (a) propagation loss as a function of femtosecond laser power, (b) mode field diameter as a function of laser power. Inset in (b) Intensity profile of the waveguide mode of the fabricated switch. Waveguide is fabricated under an angle of 58° with respect to the femtosecond laser polarization.

of about 11–12 μm similar to mode field diameter of SMF-28 of about 9.9–10.9 μm, which is necessary for low coupling losses (Fig. 9(b)). The relatively small difference in waveguide characteristics written with the two different orientations for the chosen inscription parameters suggests that the laser polarization is not as critical a parameter for waveguide inscription as it is for FLICE. Therefore, orienting the structure in such way to ensure that the microfluidics channel volume is irradiated by laser track lines perpendicular to the laser polarization is justified. It is important to keep the same orientation of the sample during the laser exposure and fabricate the waveguides and the channel in the single exposure step to ensure optimal angular and lateral alignment between the waveguides and the channel.

C. Co-Integration of Waveguides and Microfluidic Channel

Since exposing fused silica to femtosecond laser beam results in a modification of both optical and chemical properties of fused silica in the focal volume of the laser beam, co-integration of the waveguides and channel can lead to etching of the waveguides together with the channel and can cause damage to the channel walls. The way to overcome this is to start writing waveguides after some distance from the channel's wall [30]. To investigate
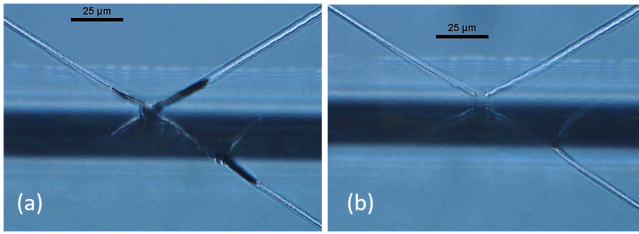
Fig. 10. Microscope images of fabricated switches: (a) Etched waveguides which are placed at the channel wall and (b) intact waveguides which are placed about 2 μm away from the channel wall to avoid their etching.

this, we write 10 TIR switches varying the separation between the waveguides and the walls of the channel. The waveguides of the first TIR switch are starting exactly at the channel wall and the waveguides of the last switch are separated 10 μm from the channel wall. It is estimated from the microscope images after the etching of the channel that if the waveguides are separated at least 2 μm from the channel, they are not etched together with the channel (Fig. 10).

V. EXPERIMENTAL RESULTS AND DISCUSSION

The switch is fabricated using the nominal values of structural parameters given in Table I. The length of the input and output waveguides is 1.7 cm to simplify the measurements. In the future, the OPS can be fabricated with shorter access waveguides to reduce the total insertion loss and overall size of the switch. The fabricated waveguides are single mode. The mode is nearly circular and has a diameter of 11.5 μm at 1550 nm (Inset in Fig. 9(b)), which allows for low loss coupling to and from single mode optical fibers. The measured coupling loss per SMF/waveguide interface is less than 1.2 dB without applying RI matching fluid and about 0.86 dB with applied RI matching liquid between the input and output fibers and waveguides. Different techniques have been reported for fabrication of more symmetrical waveguides with improved coupling efficiency to SMF-28 fibers [31], [32]. However, in this work we use a simple and robust writing scheme described in the Section IV since the focus of our work is to demonstrate the single step laser exposure method for fabricating a microfluidics-controlled optical switch in fused silica. The propagation loss in the waveguide at 1550 nm is polarization independent and about 0.5 dB/cm, as measured with the OFDR method (Fig. 9(a)). Assuming a step index profile for the waveguide RI and using the waveguide dimensions obtained from microscope images, the induced RI difference is derived to be 5×10^{3}. This value is used in the simulations in the Sections II and III.

The optical switch is experimentally characterized using a laser light source at the wavelength of 1550 nm (QPhotonics) and an optical power meter (Newport 1930-C) to detect the powers at the two outputs. The light is in- and out-coupled from the switch through edge coupled single mode optical fibers at 1550 nm (SMF-28 from Corning), as schematically presented in Fig. 1(a). The fiber to fiber transmission is measured as a reference for the insertion loss of the OPS. Index matching liquid (RI = 1.46 at

589.3 nm (D line) from Cargille, series A) is applied between the fibers for the reference measurement and fibers and waveguides for the insertion loss measurements.

First the TIR state is characterized with air in the channel. The measured insertion loss is 4.93 dB. To calculate the loss due to the reflection at the mirror only, the propagation loss contribution and the coupling loss between fibers and waveguides are subtracted from the total insertion loss. The obtained reflection loss is 1.5 dB. Since the angular misalignment in the xy plane can be eliminated when the waveguides and channel are fabricated in a single exposure step, the major contributions to the reflection loss are believed to originate from the $\pm 1°$ sidewall angle and the roughness of the channel wall.

The power at output 2 is characterized after filling the channel with RI-matching liquid. The measured insertion loss is 3.93 dB. This loss is compared with the insertion loss of a waveguide written on the same fused silica sample without the channel. The reference waveguide has the same length as the sum of input and output waveguides and it is parallel to them to ensure inscription under the same conditions. The insertion loss of the reference waveguide is 3.43 dB indicating that the excess loss due to transmission through the channel is 0.5 dB. The same value for the transmission loss was obtained after subtracting the waveguide propagation loss and the coupling losses between the fibers and waveguides from the insertion loss in the transmission state of the switch. Since the waveguides are 2 μm away from both channel sides and the RI of the liquid is equal to the RI of unmodified fused silica, the channel width is effectively about 24 μm which can lead to about 0.5 dB loss at output 2 according to the simulation results in Section II.

VI. CONCLUSION

In conclusion, we demonstrated a total internal reflection based optical switch in a fused silica substrate containing microfluidic channel and optical waveguides, both fabricated by femtosecond laser inscription. The switch actuation is performed by filling and removing RI matched liquid from the channel. The submicron precision of FLI and the possibility to define high-aspect ratio microfluidic structures with vertical sidewalls can provide the necessary accuracy for the fabrication of a low insertion loss TIR switch. The measured loss of the fabricated switch due to transmission through the channel filled with refractive index matching liquid is about 0.5 dB at a wavelength of 1550 nm. This is the minimal achievable loss as predicted from simulations for the structural parameters of the switch. The measured total internal reflection loss of the fabricated switch is 1.5 dB. This loss might be lowered further by ensuring a lower roughness of the channel wall and smaller sidewall angle.

REFERENCES

[1] R. Stabile, A. Albores-Mejia, A. Rohit, and K. A. Williams, "Integrated optical switch matrices for packet data networks," *Microsyst. Nanoeng.*, vol. 2, Jan. 2016, Art. no. 15042.

[2] Y. Silberberg, P. Perlmutter, and J. E. Baran, "Digital optical switch," *Appl. Phys. Lett.*, vol. 51, no. 16, pp. 1230–1232, 1987.

[3] T. J. Seok, N. Quack, S. Han, R. S. Muller, and M. C. Wu, "Large-scale broadband digital silicon photonic switches with vertical adiabatic couplers," *Optica*, vol. 3, no. 1, pp. 64–70, 2016.

[4] K. Suzuki *et al.*, "Low-insertion-loss and power-efficient 32 × 32 silicon photonics switch with extremely high-Δ silica PLC connector," *J. Lightw. Technol.*, vol. 37, no. 1, pp. 116–122, Jan. 2019.

[5] H. D'heer *et al.*, "Non-volatile liquid controlled adiabatic silicon photonics switch," *J. Lightw. Technol.*, vol. 35, no. 14, pp. 2948–2954, Jul. 2017.

[6] H. D'heer *et al.*, "A 16 × 16 non-volatile silicon photonic switch circuit," *IEEE Photon. Tech. Lett.*, vol. 30, no. 13, pp. 1258–1261, May 2018.

[7] H. D'heer, K. Saurav, W. Xie, C. Lerma Arce, J. Watté, and D. Van Thourhout, "Vertical liquid controlled adiabatic waveguide coupler," *Opt. Express*, vol. 26, no. 16, pp. 19877–19884, Jul. 2018.

[8] H. D'heer *et al.*, "Broadband and temperature tolerant silicon nitride liquid controlled waveguide coupler," *J. Light. Technol.*, vol. 37, no. 5, pp. 2311–2316, Feb. 2019.

[9] K. Sugioka and Y. Cheng, "Femtosecond laser processing for optofluidic fabrication," *Lab Chip*, vol. 12, no.19, pp. 3576–3589, Jul. 2012.

[10] R. Osellame, G. Cerullo, and R. Ramponi (Eds.), *Femtosecond Laser Micromachining: Photonic and Microfluidic Devices in Transparent Materials*. Berlin, Germany: Springer Verlag, 2012.

[11] L. Cerami, E. Mazur, S. Nolte, and C. B. Schaffer, *Ultrafast Nonlinear Optics*, R. Thomson, C. Leburn, D. Reid, Eds. Berlin, Germany: Springer International Publishing, 2013.

[12] F. Van Laere *et al.*, "Nanophotonic polarization diversity demultiplexer chip," *J. Lightw. Technol.*, vol. 27, no. 4, pp. 417–425, Feb. 2009.

[13] S. Kiyama, S. Matsuo, S. Hashimoto, and Y. Morihira, "Examination of etching agent and etching mechanism on femotosecond laser microfabrication of channels inside vitreous silica substrates," *J. Phys. Chem. C*, vol. 113, no. 27, pp. 11560–11566, 2009.

[14] J. E. Fouquet, "Compact optical cross-connect switch based on total internal reflection in a fluid-containing planar lightwave circuit," in *Proc. Opt. Fiber Commun. Conf. Tech. Dig. Postconference Ed. Trends Opt. Photon.*, Washington, DC, USA, 2000, vol. 37, pp. 204–206.

[15] T. Sakata, H. Togo, M. Makihara, F. Shimokawa, and K. Kaneko, "Improvement of switching time in a thermocapillarity optical switch," *J. Lightw. Technol.*, vol. 19, no. 7, pp. 1023–1027, Jul. 2001.

[16] S. Hengstler, J. J. Uebbing, P. McGuire, "Laser-activated optical bubble switch element," in *Proc. IEEE/LEOS Int. Conf. Opt. MEMS*, Waikoloa, HI, USA, Aug. 18–21, 2003, pp. 117–188.

[17] L. Shah, A. Y. Arai, S. M. Eaton, and P. R. Herman, "Waveguide writing in fused silica with a femtosecond fiber laser at 522 nm and 1 MHz repetition rate," *Opt. Express*, vol. 13, no. 6, pp. 1999–2006, Mar. 2005.

[18] A. W. Snyder and J. D. Love, "Goos-Hänchen shift," *App. Opt.*, vol. 15, no. 1, pp. 236–238, 1976.

[19] S. Ho, P. R. Herman, and J. W. Aitchison, "Single- and multi-scan femtosecond laser writing for selective chemical etching of cross section patternable glass micro-channels," *Appl. Phys. A*, vol. 106, no. 1, pp. 5–13, Jan. 2012.

[20] Y. Bellouard, A. Said, M. Dugan, and P. Bado, "Fabrication of high-aspect ratio, micro-fluidic channels and tunnels using femtosecond laser pulses and chemical etching," *Opt. Express*, vol. 12, no. 10, pp. 2120–2129, May 2004.

[21] M. Nieto-Vesperinas and J. A. Sanchez-Gil, "Light scattering from a random rough interface with total internal reflection," *J. Opt. Soc. Amer. A*, vol. 9, no. 9, pp. 424–436, 1992.

[22] C. Hnatovsky, R. S. Taylor, E. Simova, V. R. Bhardwaj, D. M. Rayner, and P. B. Corkum, "High-resolution study of photoinduced modification in fused silica produced by a tightly focused femtosecond laser beam in the presence of aberrations," *J. Appl. Phys.*, vol. 98, Jul. 2005, Art. no. 013517.

[23] C. Hnatovsky, R. S. Taylor, E. Simova, V. R. Bhardwaj, D. M. Rayner, and P. B. Corkum, "Polarization-selective etching in femtosecond laser-assisted microfluidic channel fabrication in fused silica," *Opt. Lett.*, vol. 30, no. 14, pp. 1867–1869, Jul. 2015.

[24] M. Haque, K. K. C. Lee, S. Ho, L. A. Fernandes, and P. R. Herman, "Chemical-assisted femtosecond laser writing of lab-in-fibers," *Lab Chip*, vol. 14, no. 19, pp. 3817–3829, Jul. 2014.

[25] J.-P. Bérubé and R. Vallée, "Femtosecond laser direct inscription of surface skimming waveguides in bulk glass," *Opt. Lett.*, vol. 41, no. 13, pp. 3074–3077, 2016.

[26] *Corning SMF-28 Optical Fiber Product Information*. Corning, NY, USA: Corning, Inc, Apr. 2001, pp. 1–4.

[27] B. J. Soller, D. K. Gifford, M. S.Wolfe, and M. E. Froggatt, "High resolution optical frequency domain reflectometry for characterization of components and assemblies," *Opt. Express*, vol. 13, no. 2, pp. 666–674, Jan. 2005.

[28] Cargille Laboratories, Inc., 2017, [Online]. Available: www.cargille.com

[29] M. Ams, G. D. Marshall, and M. J. Withford, "Study of the influence of femtosecond laser polarization on direct writing of waveguides," *Opt. Express*, vol. 14, no. 26, pp. 13158–13163, Dec. 2006.

[30] A. Crespi *et al.*, "Three-dimensional Mach-Zehnder interferometer in a microfluidic chip for spatially-resolved label-free detection," *Lab Chip*, vol 10, pp. 1167–1173, Feb. 2010.

[31] M. Ams, G. D. Marshall, D. J. Spence, and M. J. Withford, "Slit beam shaping method for femtosecond laser direct-write fabrication of symmetric waveguides in bulk glasses," *Opt. Express*, vol. 13, no. 15, pp. 5676–5681, Jul. 2005.

[32] R. Osellame *et al.*, "Femtosecond writing of active optical waveguides with astigmatically shaped beams," *J. Opt. Soc. Amer. B*, vol. 20, no. 7, pp. 1559–1567, 2003.